Chapter III. Functional biorecognition nanomodules

Abstract

The objective of this work is to create and characterise functional biorecognition nanomodules and define the conditions under which they form stable suspensions so that they can be subsequently used for microarraying.

It was found that 8.5mM carbonate, phosphate and citrate buffers gave the best results for the stabilisation of colloidal gold suspensions. However, when the particles were modified and for the necessary resuspension of the conjugates after centrifugation, 10mM phosphate buffer, 0.1M NaCl at pH 7.0 or 10-100mM tris-HCl buffer, 10-100mM KCl, 1%BSA, at pH 7.0-8.0 were more appropriate. High salt concentrations as well as divalent salts produced aggregation of the colloidal gold suspensions. Nevertheless, aggregation could be inhibited with 1% of BSA, which allowed to use 40mM buffer concentrations.

In this way, it was possible to produce biorecognition nanomodules with two model oligonucleotides (3' FITC-$(C)_{12}(T)_{20}(C)_{12}$-SH 5' and 3' digoxigenin-ACTTAACCGAGTCGACCGA-SH 5') that were used in a modified ELONA (Enzyme-Linked OligoNucleotide Assay) to demonstrate the efficiency of the conjugation, and in a hybridisation ELONA to demonstrate the functionality of the nanomodules. With these methods, it was possible to differentiate 4-point mutations in a target 19-mer oligonucleotide sequence. Furthermore, it was shown that the stability of the produced biorecognition nanomodules is sufficient for the purposes of mutation detection assays.

Keywords: colloidal gold, bioconjugation, nanomodules, suspension stabilisation, aggregation, thioctic acid SAMs, oligonucleotide-thiol, sandwich ELONA, hybridisation ELONA.

Introduction

Modification of colloidal particles with biomolecules has been extensively used for amplification of biorecognition reactions (Lin et al., 2000; Patolsky *et al.*, 2000; and Zhao *et al.*, 2001) or for the use of their electronic properties for biorecognition signal transduction (Powell *et al.*, 1997; Bubertret *et al.*, 2001; and Park *et al.*, 2002). Colloidal gold particles provide a convenient vehicle for the creation of biorecognition modular "libraries" (that are termed here "biorecognition nanomodules") that can be used at will for microarraying and development of biorecognition assays. They are readily available, easy to custom create (in terms of size and surface properties) and conducting, a property that provides arraying and recognition capacities. When aiming at the creation of such biorecognition nanomodules it is necessary to consider at first the nature of the colloidal gold nanoparticles. These particles are negatively charged due to adsorbed Cl^-, $AuCl_2^-$ or citrate ions left over from their synthesis procedure. When the suspension is stable, the repulsive forces of

electrostatic nature and the Van der Waals attraction forces maintain a high enough stability ratio so that the particles are essentially maintained in solution. However, changes in the ionic strength or the pH of the media will strongly influence the net charge of the colloidal particles or the degree of interaction between them, and therefore might lead to aggregation.

The DLVO theory of colloidal suspensions (Derjaguin and Landau (1941) and Verwey and Overbeek (1948)) helps to understand the nature of the interactions in colloidal suspensions. The stability of colloidal suspensions depends on the balance between the electrostatic potential (Langevin, 1908) given by:

$$V_r(H) = \frac{\pi\varepsilon_0\varepsilon r_1 r_2}{r_1 + r_2}\left[(\Psi_1 + \Psi_2)^2 \ln\{1 + \exp(\kappa H)\} + (\Psi_1 - \Psi_2)^2 \ln\{1 - \exp(-\kappa H)\}\right] \qquad \text{(Eq. III.1)}$$

where ε_0 is the permittivity in the vacuum, ε is the relative permittivity, $H = P - r_1 - r_2$ (the distance between particle surfaces = the distance between particle centres – radius of particle 1 – radius of particle 2), Ψ_1 and Ψ_2 are surface potentials of the two interacting particles, and κ^{-1} is the Debye length, and the Van der Waals attraction energy given by:

$$V_A(H) = -\frac{A}{12}\left[\frac{y}{x^2 + xy + x} + \frac{y}{x^2 + xy + x + y} + 2\ln\left\{\frac{x^2 + xy + x}{x^2 + xy + x + y}\right\}\right] \qquad \text{(Eq. III.2)}$$

where $x = H / 2r_1$, $y = r_2 / r_1$, and A is the Hamaker constant.

It can therefore be easily seen that the nature of the particle (size and Hamaker constant) is the most important parameter affecting the Van der Waals attraction forces while the conditions of the solution (e.g. ionic strength and dielectric constant) affect the electrostatic repulsive forces. The pH is a parameter that might influence both since it affects in principle the effective charge of the particles and the permittivity of the solution. The effects of modification of the surface of the particles have been studied with well-behaved model systems (Geoghegan *et al.*, 1977; Bonnard *et al.*, 1984; Brada and Roth, 1984; Morris and Saelinger, 1984; Slot and Geuze, 1985; De Waele *et al.*, 1989; Crumbliss *et al.*, 1992; O'Daly *et al.*, 1995; Elghanian *et al.*, 1997; Lyon *et al.*, 1998; Mucic *et al.*, 1998; Storhoff *et al.*, 1998; and Seelenbinder *et al.*, 1999). What is of interest here is to recognise that both the electrostatic repulsive forces and the London potential are affected due to these modifications because the effective charge and the apparent Hamaker constant are altered. However, DLVO considerations are not enough to explain these effects of surface modifications of the particles, and osmotic effects have been introduced by means of statistical thermodynamics. In many cases, quantitative predictions of stability have been made (deGennes, 1980, 1982 and 1987), although a rather detailed knowledge of the conformational multiplicity of the modifying molecules is necessary.

The above considerations also lead to the description of the kinetics of aggregation of colloidal particles. Mathematically, the rate of coagulation can be described by the stability ratio, which essentially gives the percentage of “fertile” collisions between particles, collisions that lead to aggregate formation. Again, since the stability ratio

$$W_{ij} = \frac{\beta_{ij}^{r}}{\beta_{ij}} \qquad \text{(Eq. III.3)}$$

where β^{r}_{ij} is the rapid collision frequency function with no interaction energy between particles of radii r_i and r_j and β_{ij} is the slower (observed) collision rate, the detail chosen to describe the potential function for the observed collision rate permits more or less accurate prediction of coagulation kinetics. However, it should be noted that the kinetics is also influenced by the evolution of the aggregates, and therefore an exact prediction should take these factors into account. Several works have appeared in the literature in this direction (Gardner and Theis, 1996 and Lin *et al.*, 2002).

The goal of this work is to rationally synthesise biorecognition nanomodules consisting of oligonucleotide probes conjugated to colloidal gold particles. These biorecognition modules, once characterised, will be used as nanoblocks in DNA arrays, as they will be site selectively deposited on different locations of a chip through electrophoresis. To conjugate biomolecules to colloidal gold, one takes advantage of either electronic attraction between the negatively charged colloidal gold particles and the positive sites on the protein, or adsorption between the metal surface and the hydrophobic pockets on the protein, or dative bonds between the gold and the sulfhydryl groups. The stability of the resulting conjugate suspensions depends, as mentioned above, on the kinetics and thermodynamics of the aggregation. Several authors have reported the conjugation of oligonucleotides to colloidal gold (Elghanian *et al.*, 1997; Mucic *et al.*, 1998; and Storhoff *et al.*, 1998). Here of particular importance it is to achieve the long-term stability of the suspensions.

Firstly, the conditions under which free colloidal gold suspensions are stable have been studied. As expected, the type, the pH and the concentration of the buffer play a significant role, not only because the buffer may change the nature of the ions adsorbed on the colloidal gold particles, but also because it can contribute to changes in the ionic strength of the media. It is further demonstrated that thiol-modified oligonucleotides can be conjugated to the colloidal particles, resulting in stable modified colloidal suspensions.

The modified colloids have been characterised in terms of functionality and ability to retain the biorecognition selectivity of the conjugated biomolecules with ELONA. It is demonstrated that the objective (to create “nanomodules” of biorecognition reagents) is satisfactorily achieved since the nanomodules are functional and have sufficient thermal stability (of the bond between oligonucleotides and colloidal gold particles) to allow their use under the hybridisation assay temperatures and times necessary for the detection of mutations.

Materials and methods

Materials. 20nm (21.7 ± 2.0nm) diameter colloidal gold was obtained from Sigma. The original concentration was 4.9 x 10^{11} particles mL^{-1} in about 0.01% $HAuCl_4$ suspended in 0.01% tannic acid with 0.04% trisodium citrate, 0.26mM potassium carbonate and 0.02% sodium azide as preservative. 3nm (3 ± 1nm) diameter colloidal gold was a gift from Dr. Ewen Smith. Bovine serum albumin (BSA), streptavidin-HRP, mercaptoethanol, dextran, polyethylene imine (PEI) and 3,3',5,5'-tetramethyl-benzidine (TMB) liquid substrate system for colour development (containing TMB and H_2O_2 in an slightly acidic buffer) were purchased from Sigma. Thioctic acid was bought from Aldrich. Polyethylene glycol (PEG) and cystamine were purchased from Fluka. Monoclonal antidigoxin was from Biodesign. Antidigoxigenin-HRP Fab fragments (antidig-HRP) were purchased from Roche. 3' FITC-$(C)_{12}(T)_{20}(C)_{12}$-SH 5' (FITC-oligonucleotide-thiol) and 3' digoxigenin-ACTTAACCGAGTCGA CCGA-SH 5' (dig-oligonucleotide-thiol) were from Genosys. 3' TCGGTCGACTCGGTTAAGT 5' (complementary), 3' TCGGTCGACTCGGTTAAGT-biotin 5' (biotin-labelled complementary) and 3' TCGGTGGGCTCGGGTGAGT-biotin 5' (4-mut-biotin) were from Eurogentec.

Instrumentation. Absorbance values or spectra were measured with an HP 8453 spectrophotometer or with a Molecular Devices 340PC 96-well plate reader. Chronoamperometries were performed using an AUTOLAB PGSTAT10 potentiostat in a conventional three-electrode cell, with Ag/AgCl as reference electrode and Pt as counter electrode. Fluorescence was measured with a Perkin Elmer LS-50 fluorometer or with a Nikon E600FN fluorescence microscope equipped with a Sony CCD camera.

Cystamine and thioctic acid SAMs on colloidal gold. 0.01 and 0.1M cystamine solutions were prepared in 0.1M carbonate buffer. 0.01, 0.05 and 0.1M thioctic acid solutions were prepared in 0.1M carbonate and phosphate buffer (10% ethanol). 12.5µL of each solution were put in separate eppendorfs. Afterwards, 125µL of 20nm colloidal gold commercial solution were added and mixed well. The final colloidal gold concentration was 4.5 x 10^{11} particles mL^{-1}. Absorbance spectra were monitored immediately after the mixing and after 24h. The suspensions were then centrifuged at 5000rpm and 4°C for 90min to remove unbound cystamine or thioctic acid. The supernatants were removed, and the pellets resuspended in 0.01M carbonate buffer, pH 9.3 or 10mM phosphate buffer, pH 7.0. Absorbance spectra of the resuspended solutions were monitored.

Studies of solution parameters on the stabilisation of the colloidal gold suspensions. For the effect of salts, buffers and salt/buffer combination, NaCl, KCl, KBr, KI, K_2SO_4, $CaCl_2$, $MgCl_2$ and $MgSO_4$ solutions (without and with 1% BSA), carbonate, phosphate and citrate buffers (without and with 10% ethanol, and at different pH), and several combinations of KCl with different buffers were prepared at 8.5, 40 and 85mM concentrations (without and with 1% BSA). In order to remove the original commercial buffer, 20nm colloidal gold was washed by two centrifugation steps at 5000rpm

and 4°C for 45min and resuspension in water. The 96-plate wells were filled with 85μL of the different salt and buffer solutions, and 15μL of washed colloidal gold were added and mixed well. The final colloidal gold concentration was 7.9 x 10^{11} particles mL^{-1} and the left over commercial buffer concentration was 240nM for these studies, concentration that could be neglected in comparison to the salts and buffers used. Absorbance spectra were then monitored immediately after the mixing and after 24h. For the effect of ethanol, 1mL solutions with the same 20nm colloidal gold concentration (4.9 x 10^{11} particles mL^{-1}) and different ethanol volumes (10, 30, 50, 70 and 90%) were prepared and mixed well. Absorbance spectra were then monitored immediately after the mixing and after 24h. For the effect of temperature, 200μL of a 20nm colloidal gold commercial solution (4.9 x 10^{11} particles mL^{-1}) were heated at 98°C for 1h. Absorbance spectra were monitored before and after heating.

To quantify the degree of stability of the colloidal gold or colloidal gold conjugate suspensions, the following parameter was used:

$$\% \text{ stability} = A_{523}(\text{sample}) / A_{523}(\text{blank}) \times 100 \qquad \text{(Eq. III.4)}$$

being A_{523}(sample) the absorbance at λ = 523nm of each one of the samples after mixing with salt, buffer, ethanol, or after heating, and A_{523}(blank) the absorbance at the same wavelength of a control after mixing with water or without heating. At 523nm is the maximum absorbance of the 20nm colloidal gold suspension. % aggregation (% aggregation = 100 - % stability) is also used.

Oligonucleotide conjugation to colloidal gold. 3 or 20nm colloidal gold (CG) commercial solutions were added into eppendorfs containing FITC-oligonucleotide-thiol (FOT) or dig-oligonucleotide-thiol (DOT) solutions in water and mixed well. The final colloidal gold concentrations were 0.46 x 10^{12}, 0.92 x 10^{12}, 2.31 x 10^{12}, 2.54 x 10^{12}, 3.23 x 10^{12} and 4.61 x 10^{12} particles mL^{-1} and the final oligonucleotide-thiol concentrations were 1, 1.5, 2, 3, 4 and 5μM. Mixtures were left to react for 40h at room temperature and protected from light. Afterwards, they were centrifuged twice unless otherwise mentioned at 5000rpm and 4°C for 30min. The supernatants were removed, and the pellets were resuspended in 50mM histidine buffer, pH 7.0 (for the FITC-oligonucleotide-thiol-colloidal gold conjugate) or 50mM tris-HCl buffer, 10mM KCl, pH 7.5 (for the dig-oligonucleotide-thiol-colloidal gold conjugate). Absorbance spectra of the resuspended solutions were monitored.

Characterisation of the FITC-oligonucleotide-thiol conjugation to colloidal gold (Scheme III.1). The protocol by Demers *et al.* (2000) was used. Mercaptoethanol was added to a small aliquot of the conjugate solution (12mM final concentration). The mixture was left to react for 18h at room temperature with intermittent shacking. Afterwards, it was centrifuged at 5000rpm and 4°C for 30min in order to separate the displaced oligonucleotides. The supernatant was then removed and 10-fold diluted, and the fluorescence emission was measured (excitation at 465nm and emission at 520nm).

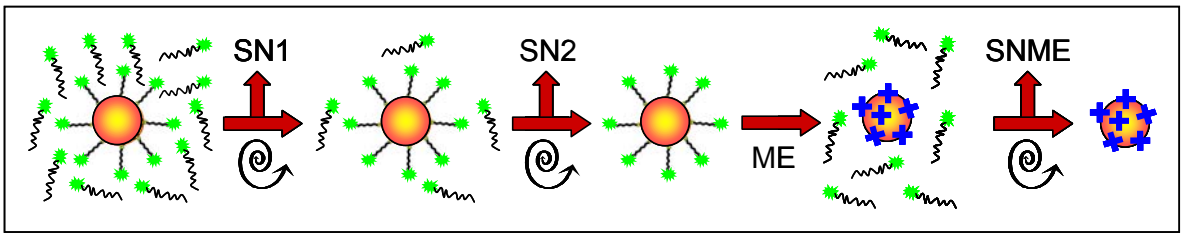

Scheme III.1. Procedure for the washing and removal of bound oligonucleotide by mercaptoethanol for the characterisation of the FITC-oligonucleotide-thiol conjugation to colloidal gold. means centrifugation. SN1: supernatant from the first washing step. SN2: supernatant from the second washing step. ME: mercaptoethanol addition. SNME: supernatant from the step of removal by mercaptoethanol.

The same experiment was used to study the stability of the modification. In this case, after three washing steps and before removal by mercaptoethanol, the sample was heated at 65°C for 1h, and an extra centrifugation step at 5000rpm and 32°C for 30min was carried out to separate the desorbed oligonucleotides. In the control, the sample was not heated but it was centrifuged. Parallel controls assured the lack of bleaching of the FITC under the same conditions.

Characterisation of the dig-oligonucleotide-thiol conjugation to colloidal gold (Scheme IIII.2).

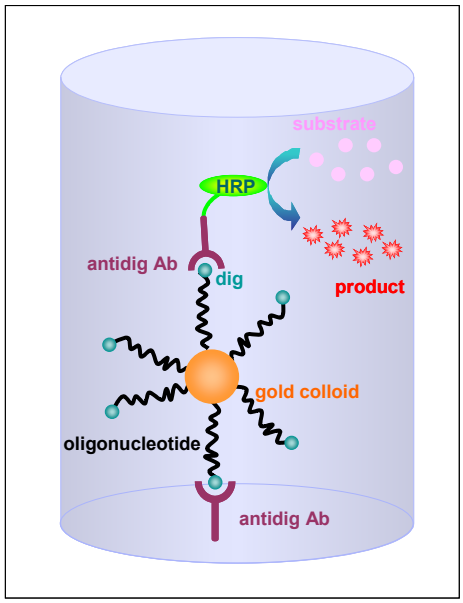

Scheme III.2. Sandwich ELONA on a well for the characterisation of the dig-oligonucleotide-thiol conjugation to colloidal gold. The well is coated by antidigoxigenin; the digoxigenin of the dig-oligonucleotide-thiol-colloidal gold conjugate recognises the antidigoxigenin; the antidig-HRP recognises the digoxigenin of the immobilised dig-oligonucleotide-thiol-colloidal gold conjugate; the HRP label reacts with its substrate to give a coloured product.

Modified ELONA with colloidal gold bioconjugates was performed. 96-well plates were coated with 50µL of an antidigoxin solution (5µg mL^{-1} in 0.01M phosphate buffer, 0.138M NaCl, 0.0027M KCl, pH 7.4). The remaining sites were blocked with 200µL of a BSA solution unless otherwise mentioned (1% in 0.05M tris-HCl buffer, 0.01M KCl, pH 7.5). 50µL of a dig-oligonucleotide-thiol-colloidal gold solution (2.94×10^{11} particles mL^{-1} in 0.05M tris-HCl buffer, 0.01M KCl, pH 7.5, with or

without 1% BSA) were incubated. FITC-oligonucleotide-thiol-colloidal gold (2.45 x 10^{12} particles mL^{-1}) was used as a control. The BSA blocking step was then repeated. 50µL of an antidig-HRP solution unless otherwise mentioned (1:2000 dilution from the commercial solution in 0.05M tris-HCl buffer, 0.01M KCl, pH 7.5, 1% BSA) were incubated. 50µL of commercial TMB liquid substrate were incubated. Each step was carried out for 1h at 37°C with stirring and protected from light. The wells were thoroughly rinsed between each step. Absorbance values were measured at 650nm.

Characterisation of the dig-oligonucleotide-thiol-colloidal gold functionality (Scheme III.3). A modified hybridisation ELONA with colloidal gold bioconjugates was performed. The protocol is the same as in the previous experiment but includes a hybridisation step after incubation with colloidal gold conjugate: 50µL of a solution of biotin-labelled complementary oligonucleotide, non-labelled complementary oligonucleotide or biotin-labelled oligonucleotide with 4-point mutations (5µg mL^{-1} in 10mM tris-HCl, 1mM EDTA, 0.3 x SSC, 2 x Denhardt's solution, pH 8.0) were incubated for 1h at 55°C with stirring and protected from light. Instead of antidig-HRP, 50µL of streptavidin-HRP (0.4µg mL^{-1} in 0.1M tris-HCl buffer, 0.1M KCl, pH 8.0, 1% BSA) were incubated for 1h at 37°C. In the wells was then added commercial TMB liquid substrate and incubated for 1h at 37°C. Between each step, the wells were thoroughly rinsed. Absorbance values were measured at 650nm.

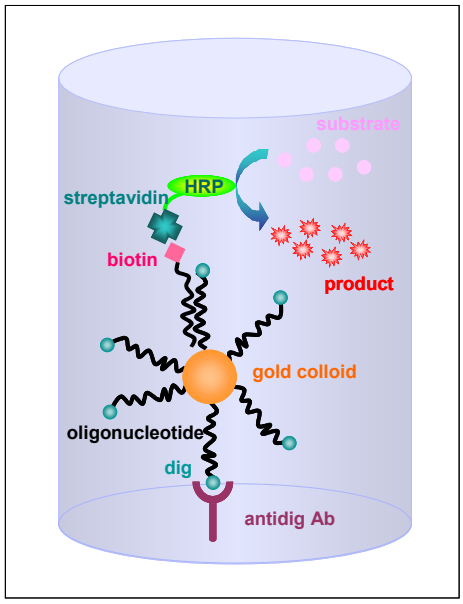

Scheme III.3. Hybridisation ELONA on a well for the characterisation of the dig-oligonucleotide-thiol-colloidal gold functionality. The well is coated by antidigoxigenin; the digoxigenin of the dig-oligonucleotide-thiol-colloidal gold conjugate recognises the antidigoxigenin; the oligonucleotide of the dig-oligonucleotide-thiol-colloidal gold conjugate hybridises with its complementary sequence; the streptavidin-HRP recognises the biotin of the complementary oligonucleotide; the HRP label reacts with its substrate to give a coloured product.

Results and discussion

Cystamine and thioctic acid SAMs on colloidal gold. Cystamine and thioctic acid SAMs on colloidal gold were tried in order to have amine or carboxylic acid functionalities on the particles and afterwards to react them with activated oligonucleotides via EDC reaction. Self-assembling of cystamine and thioctic acid (dissolved in water and 50% water : 50% ethanol, respectively) resulted in aggregation. Because several extreme concentrations were tried, one can affirm that the problem was not an inappropriate ratio between reactants. Nevertheless, as theory indicates, the media where the conjugation takes place also has an important role in the completion of a conjugation. Consequently, self-assembling was tried again in several buffers without ethanol for cystamine monolayers and with 10% ethanol for thioctic acid monolayers. Thioctic acid conjugations showed well-defined absorbance peaks at 523nm with 84 and 77% stability in carbonate and phosphate buffer, respectively, being the carbonate buffer slightly better. After 24 hours the stability percentages were 78 and 71%, suggesting a slow aggregation process. On the other hand, aggregation appeared when using cystamine in any buffer. In fact, Weisbecker *et al.* (1996), in their study of SAMs on gold colloids, reported that flocculation is a common phenomenon especially with short length alkanethiols. In the case of cystamine, the inversion of the charge of the particles' surface might be the reason for aggregation.

Thioctic acid / colloidal gold suspensions were washed in order to remove the unbound thioctic acid molecules, and several buffers were used to see if the suspensions were stable after the centrifugation step. Figure III.1 shows the spectra of the suspensions before the washing step and after resuspension of the pellets in carbonate and phosphate buffer.

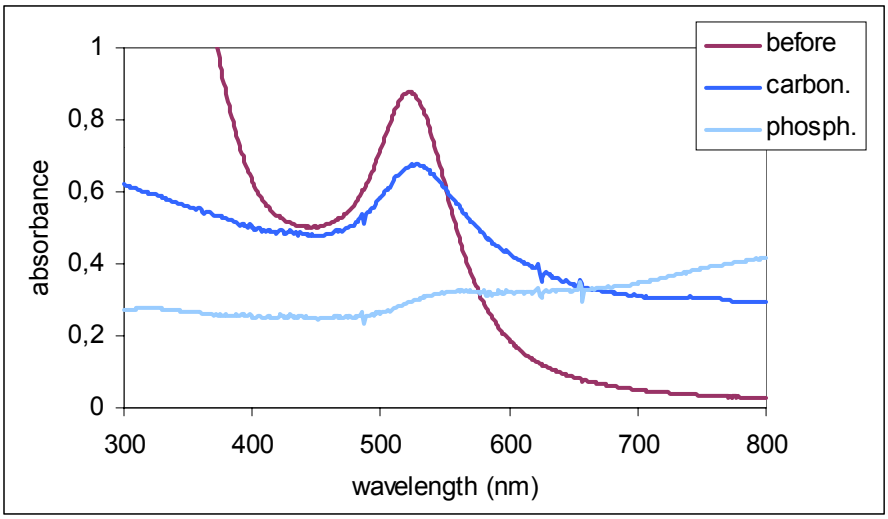

Figure III.1. Absorbance *vs.* wavelength for thioctic acid-colloidal gold suspensions (4.5×10^{11} particles mL^{-1}) before and after washing and resuspension in 0.01M carbonate buffer, pH 9.3 or 0.01M phosphate buffer, pH 7.0.

In carbonate buffer, a well-defined absorbance peak is observed at 523nm, although the 22% aggregation is evident. The suspension was not stable in phosphate buffer, and aggregates could be observed. Although neither carbonate nor phosphate buffers destabilised the colloidal gold suspension when thioctic acid was added, the election of the resuspension buffer after the centrifugation step was decisive, only carbonate buffer being useful. Although in this experiment, only one washing step was performed, in subsequent experiments (conjugations of oligonucleotides to colloidal gold) more than one washing steps were required to completely remove all the unbound material. If more than one washing steps are needed, a compromise should be taken between removal of unbound material and stability of the conjugate suspension, since repeated centrifugations were observed to destabilise the suspension.

As mentioned above, cystamine and thioctic acid SAMs on colloidal gold were attempted as a means to have functionality-modified colloidal gold to subsequently react with activated oligonucleotides via EDC reaction. However, this strategy was eventually abandoned in favor of direct self-assembling of oligonucleotide-thiol monolayers on colloidal gold particles, not only because of aggregation but also because of the EDC step, only 15% efficient.

Studies of solution parameters on the stabilisation of the colloidal gold suspensions. The conditions under which colloidal gold suspensions are stable were studied in order to proceed with the rational colloidal gold conjugation with oligonucleotides. All gold colloids offered by Sigma are produced by a modified method of Slot and Geuze (1985) and contain about 0.01% $HAuCl_4$, 0.01% tannic acid, 0.04% trisodium citrate, 0.26mM potassium carbonate and 0.02% sodium azide as preservative. Consequently, colloidal gold particles are supposed to have Cl^-, $AuCl_2^-$, citrate ions and tannic acid on their surface. In order to avoid the effects of the original commercial buffer, the colloidal gold suspensions were centrifuged twice, and after addition in the corresponding solutions, the total concentration of the original commercial buffer was only 240nM, negligible compared to 0.85-85mM salts and buffers concentrations used in this work. As the stabilisation of colloidal gold suspensions was desired to further modify the colloidal gold particles with different self-assembled chemistries, buffers, salts and combinations of both were prepared in the presence or not of 10% ethanol.

Table III.1 shows the salt effect in the colloidal gold suspensions. In this and the following tables, stability is considered when the stability percentage is higher than 85%, intermediate stability when the stability percentage is between 50 and 85%, and instability when the stability percentage is below 50%. If no BSA was present, all salt solutions at 85mM concentration destabilised the suspensions because the high ionic strength resulted in the screening of the supposedly negatives charges that are on the particles' surface, which arise from the synthesis procedure and help to maintain the stability of the suspensions. Nevertheless, when lower concentrations were used, only the salts with divalent positive counterions destabilised the colloidal gold suspensions, as expected

since the colloidal gold particles are negatively charged. The results of the stability of the colloidal gold suspensions in NaCl, KCl and KBr solutions reflect that the experimental critical coagulation concentration for these systems is between 8.5 and 8.5mM of electrolyte. Whereas suspensions in K_2SO_4 behave as in NaCl, KCl and KBr, suspensions in salt solutions with divalent cations are destabilised at lower ionic strengths, the experimental critical coagulation concentration being below 0.85mM, making obvious the "chemical" effects of the divalent cations, which can effectively reverse the surface charge. An evident further stabilising effect was observed when 1% BSA was present in the suspensions. In fact, BSA is expected to spontaneously adsorb on the surface of colloidal gold particles. It has an isoelectric point of approximately 5, and at the pH of the media (about 6) has a weak net negative charge that contributes to maintain the anionic atmosphere and avoid aggregation. This stabilising effect is expected when polymeric effects are taken into account. However, the effect might simply be "chemical" (i.e. lyophilisation of the lyophobic gold particles).

Table III.1. Colloidal gold suspension stability (✓), instability (×) or intermediate stability (⊙) in salt solutions at different concentrations without and with 1% BSA after 24h.

SALT	No BSA			1% BSA		
	85mM	8.5mM	0.85mM	85mM	8.5mM	0.85mM
NaCl	×	✓	✓	✓	✓	✓
KCl	×	✓	✓	✓	✓	✓
KBr	×	✓	✓	✓	✓	✓
K_2SO_4	×	✓	✓	✓	✓	✓
$CaCl_2$	×	×	×	⊙	✓	✓
$MgCl_2$	×	×	×	⊙	✓	✓
$MgSO_4$	×	×	×	⊙	✓	✓

Table III.2 summarises the results for the stability of colloidal gold suspensions in different buffers, at different pH and concentrations, without and with 10% ethanol. When using 85 or 40mM final buffer concentration, colloidal gold aggregated, independently of the pH. Only citrate buffer at 40mM and at the lowest pH (2.5) showed an intermediate destabilisation effect. At 8.5mM, any buffer could be used without destabilising the colloidal gold suspensions at any pH. Again, the general effect of buffer concentration can be explained in terms of charge screening and a shorter Debye length at higher concentrations, which leads to aggregation. Regarding the effect of ethanol, no differences were observed between suspensions with or without ethanol after 24 hours, although when absorbance spectra were measured immediately after mixing, suspensions without ethanol were slightly more stable (*results not shown*). Despite the shorter Debye length due to the lower dielectric constant of ethanol compared to water (24.3 *vs.* 80.0F m^{-1}), both the electrostatic repulsion between particles and the apparent Hamaker constant allow the stability of the suspension.

Table III.2. Colloidal gold suspension stability (✓), instability (×) or intermediate stability (⊙) in buffers at different pH and concentrations without and with 10% ethanol after 24h.

BUFFER	No ethanol						10% ethanol					
	85mM		40mM		8.5mM		85mM		40mM		8.5mM	
carbonate	11.5	×	10.5	×	8.5	✓	11.0	×	10.5	×	9.5	✓
	10.5	×	9.5	×	7.5	✓	10.5	×	10.0	×	7.0	✓
	9.5	×	9.0	×	7.0	✓	9.5	×	9.5	×	7.0	✓
phosphate	7.0.	×	7.5	×	7.0	✓	7.0.	×	7.5	×	7.0	✓
	6.5	×	6.5	×	6.5	✓	6.5	×	6.5	×	6.5	✓
	5.5	×	6.0	×	6.0	✓	6.0	×	6.0	×	6.0	✓
citrate	6.0	×	6.0	×	5.5	✓	5.5	×	6.0	×	6.0	✓
	4.0	×	4.5	×	4.5	✓	4.0	×	4.5	×	4.5	✓
	2.5	×	2.5	⊙	2.5	✓	2.5	×	2.5	⊙	3.0	✓

KCl was added to different buffers (without and with 1% BSA) at 85mM concentration to make sure that colloidal gold suspensions were stable under saline conditions, needed for electrochemistry. Whereas colloidal gold suspensions were not stable in any of the saline buffers without BSA, the presence of 1% of this protein resulted in stabilisation (Table III.3). Again, the protective action of BSA was demonstrated, as colloidal gold suspensions could be stable even under 85mM KCl concentration, result that correlates with the two previous independent experiments (effect of salts and effect of buffers).

Table III.3. Colloidal gold suspension stability (✓), instability (×) or intermediate stability (⊙) in buffers at different pH and concentrations with 85mM KCl without and with 1% BSA after 24h.

85mM KCl BUFFER	No BSA				10% BSA			
	40mM		8.5mM		40mM		8.5mM	
carbonate	10.5	×	9.0	×	10.0	✓	8.5	✓
	10.0	×	7.5	×	9.5	✓	7.5	✓
	9.5	×	7.0	×	9.0	✓	7.0	✓
phosphate	7.0	×	6.5	×	7.0	✓	7.0	✓
	6.5	×	6.0	×	6.5	✓	6.5	✓
	5.5	×	5.5	×	5.0	✓	5.5	✓
citrate	6.0	×	6.0	×	6.0	✓	6.0	✓
	4.0	×	4.5	×	4.5	✓	4.5	✓
	2.0	×	2.5	×	2.5	✓	4.0	✓

The stability of the colloidal gold suspension in different percentages of ethanol was studied to see if the presence of this solvent (necessary to dissolve the thioctic acid and consequently, to form thioctic acid SAMs on gold) had any aggregation effect on the colloidal gold. Initially, the colour of all the samples was pink and the absorbance spectra showed well-defined peaks at 523nm (Figure III.2). Although all samples seem stable, the sample with 90% ethanol showed an increase in the absorbance around 620nm and a decrease of the 523nm peak absorbance, corresponding to 22% aggregation.

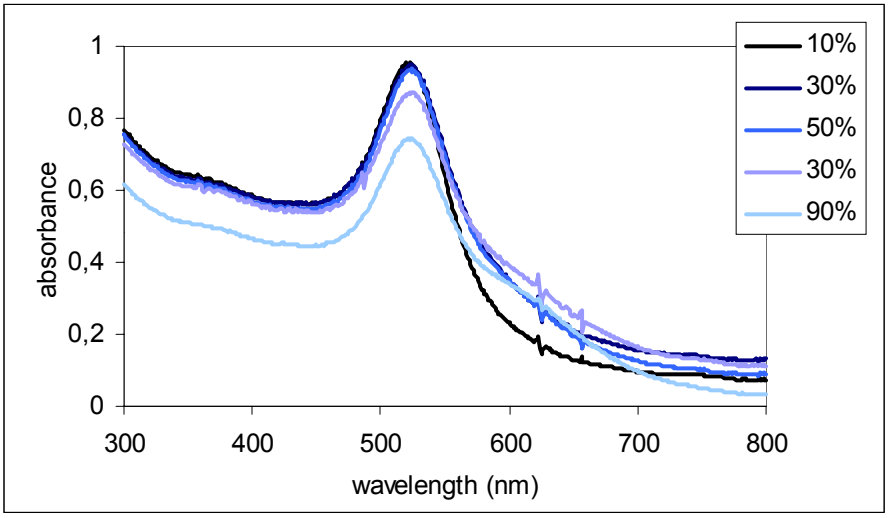

Figure III.2. Absorbance *vs.* wavelength for colloidal gold suspensions with different ethanol content.

After 24h, only the samples with 10 and 30% ethanol content were stable. The samples with higher ethanol content showed a darker purple colour as the percentage of ethanol increased (Figure III.3), reflected by the absorbance decrease at 523nm and the absorbance increase at 620nm.

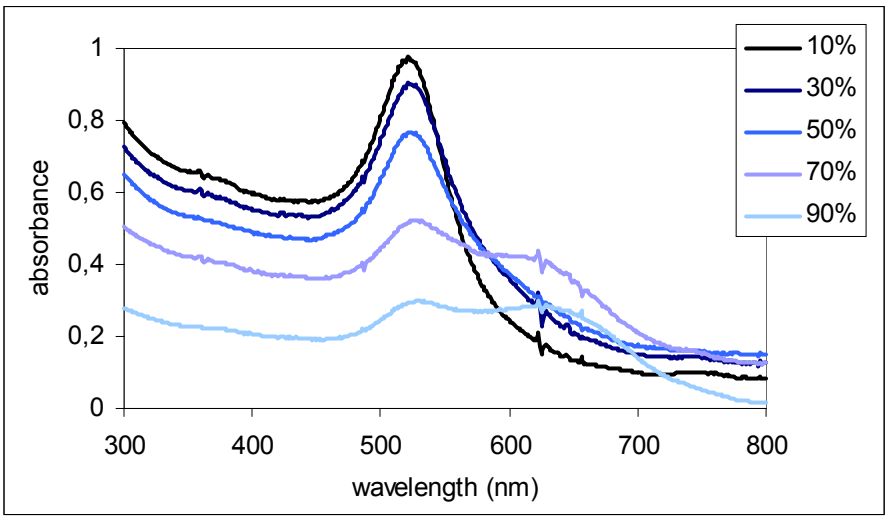

Figure III.3. Absorbance *vs.* wavelength for colloidal gold suspensions with different ethanol content after 24h.

In this case, the aggregation was 21, 46 and 69% for 50, 70 and 90% ethanol content, respectively. As mentioned above, this aggregation effect was expected because of the lower dielectric constant of ethanol, which shortens the Debye length. It is not easy to account for the slow kinetics of aggregation in ethanol. Theory suggests that for the conditions under investigation, doublet formation times should be of the order of magnitude of seconds. Agreement with theory should be examined by the explicit integration of the stability ratio given as

$$W_{ij} = 2a\int_{2a}^{\infty} \frac{exp(\Phi / kT)}{r^2 G(r)} dr \qquad \text{(Eq. III.4)}$$

where *a* is the particle radius, *r* is the centre-to-centre particle separation, $\frac{\Phi}{kT}$ is the dimensionless interparticle interaction potential, and *G*(*r*) is the probability density, of which the doublet formation depends.

The thermal stability of the colloidal gold suspension was studied to ensure that heating does not provoke any aggregation, as the biorecognition modules have to be stable during the hybridisation step. Although hybridisation is usually performed at lower temperatures, 98°C were used to study the thermal stability of colloid suspensions under extreme conditions. The absorbance spectrum for the colloidal gold solution after 1h at 98°C showed a well-defined peak at 523nm with only 19% aggregation. The well-defined peak indicated that the stability of the suspension was adequate.

Oligonucleotide conjugation to colloidal gold. The conjugation of FITC-oligonucleotide-thiol (3μM) to colloidal gold (2.31 x 10^{12} particles mL^{-1}) was performed in triplicate and the peak absorbance at 523nm showed only 3% standard deviation, demonstrating the high reproducibility of the stability of the conjugate suspension. The conjugations of dig-oligonucleotide-thiol (1.5μM) to colloidal gold (2.54 x 10^{12} particles mL^{-1}, 3 or 20nm in diameter) were performed in quadruplicate. Whereas peak absorbance values from 20nm colloidal gold conjugates showed 11% standard deviation, the standard deviation from 3nm colloidal gold conjugates was 22%, suggesting a lower reproducibility. Additionally, 3nm colloidal gold conjugates showed 32% lower peak absorbance than 20nm colloidal gold conjugates, suggesting a partial aggregation effect. Although 8.5mM carbonate, phosphate and citrate buffers gave the best results for the stabilisation of colloidal gold suspensions, 10mM phosphate buffer, 0.1M NaCl at pH 7.0 and 10-100mM tris-HCl buffer, 10-100mM KCl, 1%BSA, at pH 7.0-8.0 provided better results for resuspension of the conjugates.

Characterisation of the FITC-oligonucleotide-thiol conjugation to colloidal gold (Scheme III.1). Fluorescence measurements demonstrated that oligonucleotide solutions did not emit any fluorescence after their conjugation and washing (to remove unbound oligonucleotides). This effect indicated either the presence of fluorescence quenching or the non-successful conjugation. In order to characterise the conjugation by other methods, the bound oligonucleotides were removed from

the gold particles using mercaptoethanol and their fluorescence was measured, following the procedure of Demers *et al.* (2000). The aforementioned fluorescence quenching is due to the fluorescence resonance energy transfer (FRET) between the FITC and the gold. In the FRET, the FITC moiety (donor) is excited by absorption of a photon, but instead of emitting a fluorescence photon, the excitation is transferred by electronic coupling to the colloidal gold particle (acceptor). The result of this exchange is an excited acceptor and a ground state donor. In signal terms, the result is no fluorescence. Figure III.4 shows the fluorescence values from the supernatants corresponding to two washings and the removal by mercaptoethanol of five conjugations using different colloidal gold concentrations. As expected, the fluorescence values from the washing steps increased as colloidal gold concentration decreased, due to the less colloidal gold surface available for conjugation, and this effect was much more evident for the first washing than for the second one. The fluorescence values from the removal step showed the opposite trend because the higher the colloidal gold concentration, the higher the concentration of previously bound oligonucleotides. The total sum of the fluorescence emitted by the supernatants for each colloidal gold concentration was not significantly different between conjugations (8.1% standard deviation), which indicates a high reproducibility of the assay. In subsequent dig-oligonucleotide-thiol conjugations to colloidal gold, colloidal gold concentrations close to 2.31 x 10^{12} particles mL^{-1} were used, since Figure III.4 shows that for this concentration, the amount of oligonucleotide bound to the gold particles is significantly higher than the amount of free oligonucleotide that could be still present in the solution.

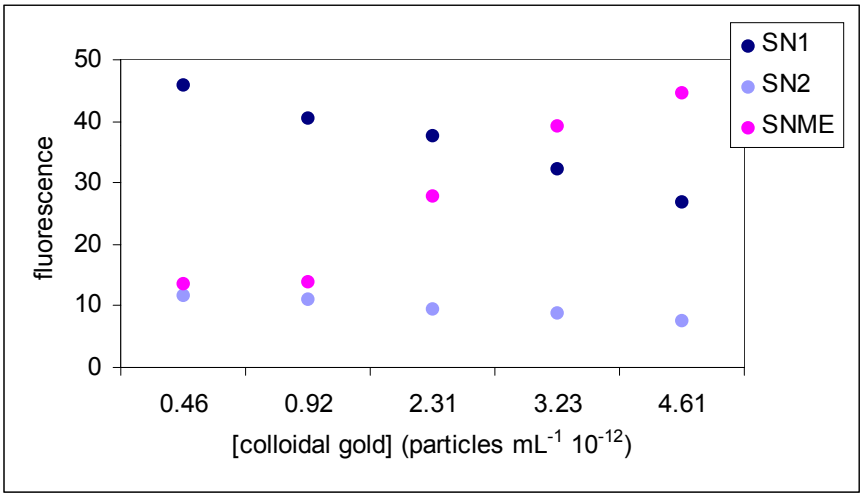

Figure III.4. Fluorescence emitted at 520nm by SN1, SN2 and SNME in the FITC-oligonucleotide-thiol-colloidal gold conjugate characterisation by mercaptoethanol for different colloidal gold concentrations and the same FITC-oligonucleotide-thiol concentration (3μM) (*see Scheme III.1*).

Figure III.5 shows the fluorescence values from the supernatants corresponding to five washings and the removal by mercaptoethanol of five conjugations using different FITC-oligonucleotide-thiol concentrations. Previous experiments with only two washing steps showed an increasing trend in the fluorescence emitted by removed oligonucleotide supernatants as the oligonucleotide concentration used in the conjugation increased. This would seem to indicate that at higher

oligonucleotide concentrations, the modification was more efficient due to displacement of the equilibrium towards the adsorbed state. However, it was postulated that the colloidal gold conjugate was not completely free of unbound FITC-oligonucleotide-thiol molecules. For this reason, more washing steps were carried out. Five washing steps were chosen because at the fifth centrifugation step, aggregates started to appear at the bottom of the eppendorfs. After five washings, the fluorescence emitted by the removed oligonucleotide supernatants (SNME) did not show any trend, demonstrating that the amount of oligonucleotide bound to the colloidal gold surface was the same independently of the initial oligonucleotide concentration. Additionally, from the SNME values, the surface coverage of bound oligonucleotides could be calculated assuming that no FITC bleaching occurred and essentially monodispersed gold. It was determined to be 14.87pmol cm^{-2}, or 159 oligonucleotides per particle, which corresponds to 37% coverage of the surface. Although it cannot be ruled out the possibility that the mercaptoethanol has not completely displaced all the oligonucleotides, it seems unlikely.

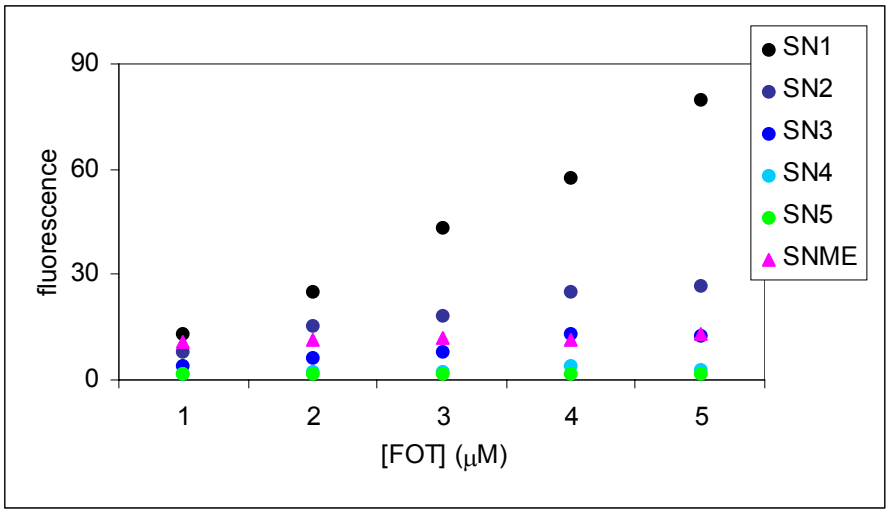

Figure III.5. Fluorescence emitted at 520nm by SN1, SN2, SN3, SN4, SN5 and SNME in the FITC-oligonucleotide-thiol-colloidal gold conjugate characterisation by mercaptoethanol for the same colloidal gold concentration (2.45 x 10^{12} particles mL^{-1}) and different FITC-oligonucleotide-thiol concentrations.

Characterisation of the dig-oligonucleotide-thiol conjugation to colloidal gold (Scheme III.2). Figure III.6 shows the absorbance results for the sandwich ELONA with dig-oligonucleotide-thiol-colloidal gold and FITC-oligonucleotide-thiol-colloidal gold used as a control (with 20nm colloidal gold). In the "total" set, the assay with dig-oligonucleotide-thiol-colloidal gold yield a coloured solution and the assay with FITC-oligonucleotide-thiol-colloidal gold did not produce any significant response different from the blank (set "no HRP"), demonstrating that the Scheme III.2 assay was valid. The "no colloid" set, which corresponds to the system without colloidal gold conjugate and which did not show any significant response, demonstrates that the antidig-HRP did not adsorb non-specifically on the BSA or on the antidigoxin coating. The bars associated to the FITC-oligonucleotide-thiol-colloidal gold conjugate present values close to the blanks, which indicates

that the antidig-HRP did not adsorb non-specifically on the colloidal gold conjugates. Consequently, the absorbance values are entirely due to the dig-antidig recognition. These observations lead to the conclusion that the dig-oligonucleotide-thiol conjugation to colloidal gold was successful and that the digoxigenin label was functional (able to recognise the antidigoxin of the coated surface and the antidig-enzyme). Comparing the "total" and the "no coat" sets, the bars associated to the dig-oligonucleotide-thiol-colloidal gold conjugate decreased when there was not antidigoxin on the well surface, and this effect was more pronounced when there was BSA in the conjugate solution. If there is not BSA in the conjugate solution, the conjugate adsorbs non-specifically on the non-coated well because this well is coated by BSA (from the first blocking step) and the tendency of the conjugate is to adsorb on this protein. Therefore, BSA in the conjugate suspension has both a stabilisation effect and a protective effect against non-specific adsorption. The results also show that an additional coating BSA step was not necessary.

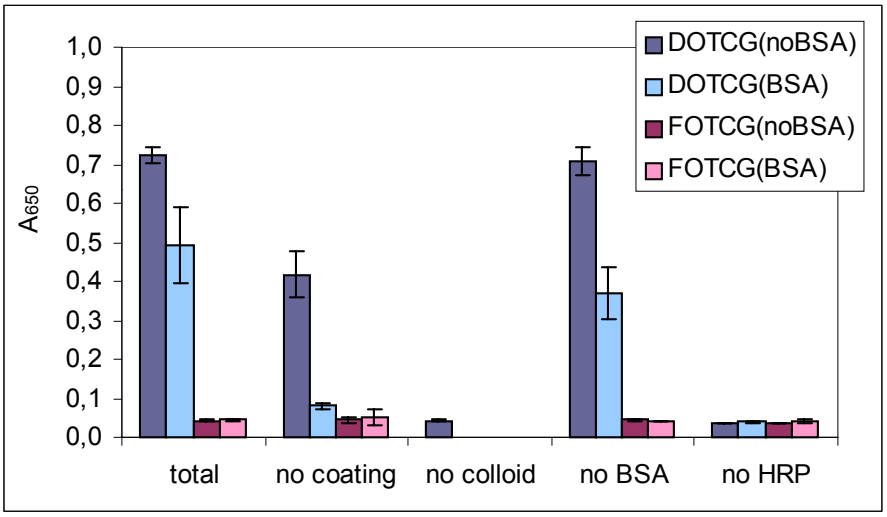

Figure III.6. Absorbance at 650nm obtained in the sandwich ELONA for the dig-oligonucleotide-thiol-colloidal gold (20nm colloidal gold) conjugate characterisation; total: system as depicted in Scheme III.2; no coating: blank without antidigoxigenin on the surface; no colloid: blank without conjugate; no BSA: blank without the blocking step; no HRP: blank without antidig-HRP. FITC-oligonucleotide-thiol-colloidal gold conjugate was used as a control.

Despite the partial aggregation of the suspensions of dig-oligonucleotide-thiol conjugated to 3nm colloidal gold, sandwich ELONA was also carried out with these conjugates. Figure III.7 compares the results for both types of conjugates, with 3 and 20nm colloidal gold. The absorbance obtained in the "total" set and the low absorbance values for the controls and blanks ("no colloid" and "no HRP" sets) demonstrate the effectiveness of both conjugations. However, the 3nm colloidal gold conjugates present lower absorbance values for the "total" system (76% of the corresponding value for the 20nm colloidal gold conjugate). Regarding the reproducibility of the functionality assay, whereas the assay with 20nm colloidal gold conjugates has a standard deviation of 6%, in the assay with 3nm colloidal gold conjugates the standard deviation is of 14% in accordance with the conjugation results for the colloids of this size.

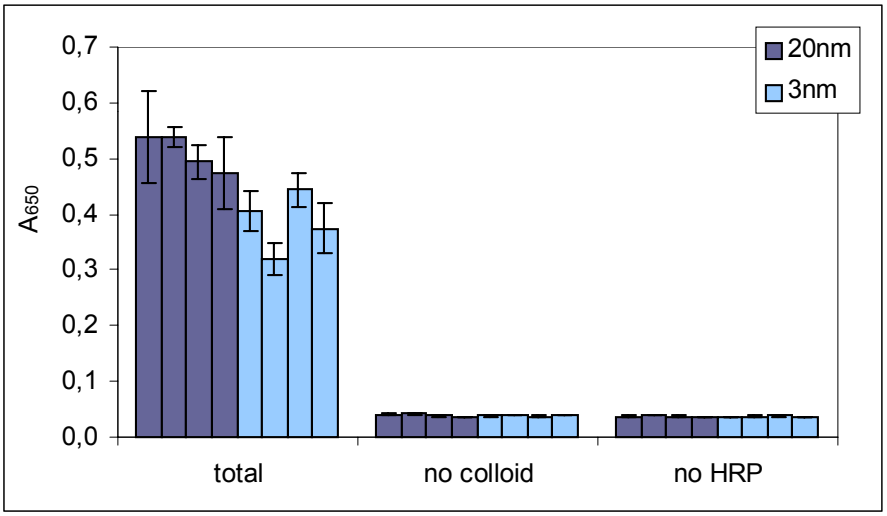

Figure III.7. Absorbance at 650nm obtained in the sandwich ELONA for the dig-oligonucleotide-thiol-colloidal gold (3 and 20nm colloidal gold) conjugate characterisation; total: system as depicted in Scheme III.2; no colloid: blank without conjugate; no HRP: blank without antidig-HRP.

In order to find the best blocking agent to avoid the non-specific adsorption of the dig-oligonucleotide-thiol-colloidal gold conjugate on the 96-well plate, a sandwich ELONA was performed using 1% BSA, PEG, PEI, dextran or glycerol in the dig-oligonucleotide-thiol-colloidal gold conjugate solution. As PEI provoked the aggregate formation, this polymer was not used as blocking agent in subsequent assays. The best results, i.e. higher absorbance values from the "total" set and lower absorbance values from the "no coating" set (*results not shown*), were obtained with BSA as blocking agent. Consequently and also due to the results obtained in the studies of the stability of colloidal gold suspensions, 1% of BSA was used in the dig-oligonucleotide-thiol-colloidal gold conjugate solutions in subsequent experiments.

Characterisation of the dig-oligonucleotide-thiol-colloidal gold functionality (Scheme III.3). Figure III.8 shows the results for the hybridisation ELONA with dig-oligonucleotide-thiol-colloidal gold and FITC-oligonucleotide-thiol-colloidal gold as a control. The dig-oligonucleotide-thiol-colloidal gold bar for the "total" set, significantly different from the rest of bars, demonstrated the hybridisation event with the dig-oligonucleotide-thiol-colloidal gold conjugate. The set associated to the system without colloidal gold conjugate presents a value close to the blanks ("no HRP"), demonstrating that the streptavidin-HRP did not adsorb non-specifically on BSA or on the antidigoxin coating. The set corresponding to the system without the hybridisation oligonucleotide presents values close to the blanks, which proves that the streptavidin-HRP did not adsorb non-specifically on the colloidal gold conjugates. As expected, the bars associated to the FITC-oligonucleotide-thiol-colloidal gold conjugate also present values similar to the blanks, because this conjugate has no digoxigenin and consequently, it cannot be immobilised on the antidigoxin-coated surface. All the controls and blanks prove that the absorbance value in the "total" set with dig-oligonucleotide-thiol colloidal gold is entirely due to the biotin-streptavidin recognition from oligonucleotides hybridised to colloidal gold conjugates. These results indicated that the

oligonucleotides conjugated to the colloidal gold are functional, i.e. able to recognise their complementary sequence. This experiment also included the hybridisation with other sequences: the fully complementary sequence without the biotin label ("no biotin" set) and the labelled oligonucleotide sequence with 4-point mutations ("4-mut" set). The low absorbance value for the hybridisation with the oligonucleotide with 4-point mutations compared to the absorbance value for the hybridisation with the fully complementary sequence showed the sensitivity of the assay, which is able to detect 4 mutations in 19-mer oligonucleotides working at 55°C. The experiment with the non-labelled complementary oligonucleotide shows that the streptavidin-HRP did not adsorb non-specifically on the complementary oligonucleotide.

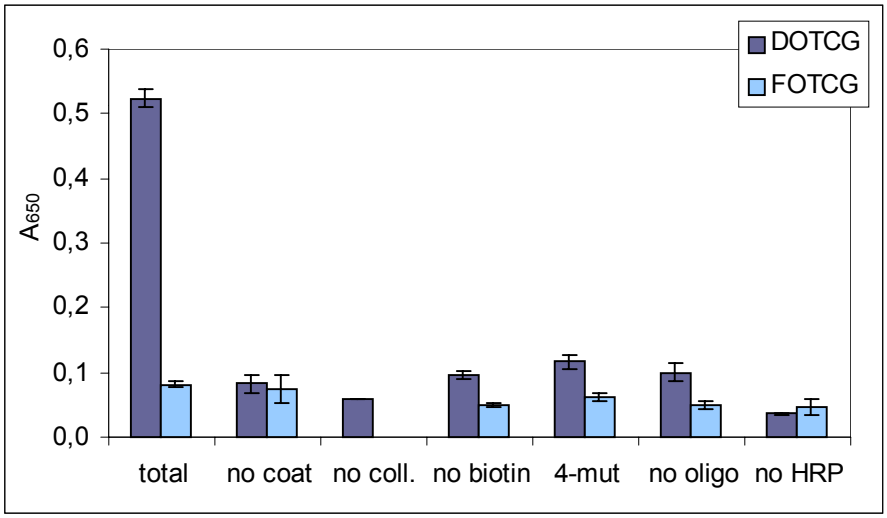

Figure III.8. Absorbance at 650nm obtained in the hybridisation ELONA for the dig-oligonucleotide-thiol-colloidal gold (20nm colloidal gold) conjugate functionality characterisation; total: system as depicted in Scheme III.3; no coating: blank without antidigoxigenin on the surface; no coll.: blank without conjugate; no biotin: blank with non-labelled complementary oligonucleotide; 4-mut: blank with biotin-labelled oligonucleotide with 4-point mutations; no oligo: blank without complementary oligonucleotide; no HRP: blank without streptavidin-HRP. FITC-oligonucleotide-thiol-colloidal gold conjugate was used as a control.

Oligonucleotide-colloidal gold thermal stability. The thermal stability of the biorecognition nanomodules, i.e. of the conjugation between oligonucleotides and colloidal gold, was studied, since the biomodules have to be stable under hybridisation temperatures. Firstly, FITC-oligonucleotide-thiol thermal stability was studied in order to ensure that fluorescence does not decay with heat. FITC-oligonucleotide-thiol fluorescence did not vary significantly with heating, proving the stability of this fluorescent moiety with temperature (*results not shown*). As FITC-oligonucleotide-thiol and colloidal gold were stable with temperature, the effect observed in the FITC-oligonucleotide-thiol-colloidal gold conjugate thermal stability, if any, had to be due to the desorption of the fluorescent oligonucleotides from the gold particle. The absorbance spectra demonstrated that the conjugate suspension did not aggregate with heating (*results not shown*). Table III.4 shows the fluorescence values for the sample and the control after three washing steps, heating and removal by mercaptoethanol.

Table III.4. Fluorescence emitted at 520nm by the supernatants from the three washings, from heat + centrifugation or only centrifugation, and from removal by mercaptoethanol.

	1st washing	2nd washing	3rd washing	After 1h	After ME	Total
Sample (heat + centrifugation)	68.5 ± 6.7	41.2 ± 1.3	15.8 ± 3.1	8.8 ± 2.5	11.1 ± 3.0	145.4 ± 16.6
Control (centrifugation)	68.6 ± 2.1	45.8 ± 6.7	13.2 ± 0.8	5.9 ± 1.0	12.7 ± 2.0	146.2 ± 12.6

The sample and the control fluorescence balances close, as indicate the total sums of the fluorescence emitted, with an experimental error of 10%. Comparing the "After 1h" values, there is a 32.9% oligonucleotide desorption from the colloid, however the experimental error in this column is 23.8%. Comparing the "After ME" values, there is a 12.6% oligonucleotide desorption from the colloid, the experimental error in this column being 21.0%. Consequently, there is between 12.6 and 32.9% oligonucleotide desorption from the colloid due to heating, but the experimental error is considerable. The group is working on new chemistries to attach the oligonucleotides to the colloidal gold particles, which may confer stronger or more bonds between DNA and colloids, and would overcome the problem of thermal stability of the interaction. Nevertheless, despite the partial oligonucleotide desorption from the colloid, the biorecognition modules have demonstrated to be functional in ELONA hybridisations.

Conclusions

The conditions under which colloidal suspensions are stable (no aggregation occurs) have been established. It was found that 8.5mM carbonate, phosphate and citrate buffers gave the best results for the stabilisation of colloidal gold suspensions. However, 10mM phosphate buffer, 0.1M NaCl at pH 7.0 or 10-100mM tris-HCl buffer, 10-100mM KCl, 1%BSA, at pH 7.0-8.0 provided better results for resuspension of the conjugates. The study of several parameters on the stability of colloidal gold suspensions, and the observation of the aggregation after 24h in some experiments, showed that aggregation could be a slow process and that can be inhibited when using protective agents, like BSA in the colloidal gold suspension.

Two model oligonucleotides, with FITC and digoxigenin as labels, were conjugated to 20nm colloidal gold, resulting in stable and reproducible colloidal gold suspensions, with 3% standard deviation for FITC-oligonucleotide-thiol-colloidal gold conjugates and 11% standard deviation for dig-oligonucleotide-thiol-colloidal gold conjugates. When 3nm colloidal gold was used, both the stability and the reproducibility of the conjugate suspension were lower (32% lower peak absorbance and 22% standard deviation). The effectiveness of the conjugations was demonstrated

by fluorescence for FITC-oligonucleotide-thiol-colloidal gold conjugates and by sandwich ELONA for dig-oligonucleotide-thiol-colloidal gold conjugates. BSA was found to act as an effective blocking and protecting agent in the oligonucleotide-thiol-colloidal gold conjugate suspensions and assays. Hybridisation ELONA demonstrated the functionality of the bionanomodules and the ability to differentiate 4-point mutations in 19-mer oligonucleotide sequences.

The thermal stability corresponding to the interaction of colloidal gold with oligonucleotide-thiol was studied by fluorescence methods in order to know if the nanomodules were suitable for hybridisation at high temperatures. Between 12.6 and 32.9% of FITC-oligonucleotide-thiol desorbed from the colloids surface after 1 hour at 65°C. Nevertheless, the experimental error is considerable and the biorecognition modules still worked in hybridisation assays.

The stability of the oligonucleotide-colloidal gold conjugate suspensions, the functionality of these conjugates, and the thermal stability of the modification or interaction between the two components (oligonucleotides and colloidal gold), make the rationally designed biorecognition nanomodules suitable for use in DNA sensors. By taking benefit from the colloidal gold properties, these conjugates will be selectively electrodeposited on arrays and the hybridisation event will be detected by electrochemical techniques, providing a promising integrated approach for DNA arrays, competitive with the current arraying technologies.

References

Bonnard C., Papermaster D.S., and Kraehenbuhl, J.-P., in *Immunolabelling for Electron Microscopy*, ed. Elsevier, New York, USA, **1984**, pp. 95-111.

Brada D. and Roth J., *Anal. Biochem.*, **1984**, 142, 79.

Crumbliss A.L., Perine S.C., Stonehuerner J., Tubergen K.R., Zhao J., Henkens R.W., and O'Daly J.P., *Biotechnol. Bioeng.*, **1992**, 40 (4), 483.

deGennes P.-G., *Macromolecules*, **1980**, 13, 1069.

deGennes P.-G., *Macromolecules*, **1982**, 15, 492.

deGennes P.-G., *Adv. Colloid Interface Sci.*, **1987**, 27, 189.

Demers L.M., Mirkin C.A., Mucic R.C., Reynolds R.A., Letsinger R.L., Elghanian R., and Viswanadham G., *Anal. Chem.*, **2000**, 72 (22), 5535.

Derjaguin B.V. and Landau L., *Acta Physiochim.*, **1941**, 14, 633.

De Waele M., Renmans W., Segers E., De Valck V., Jochmans K., and Van Camp B., *J. Histochem. Cytochem.*, **1989**, 37 (12), 1855.

Dubertret B., Calame M., and Libchaber A.J., *Nature Biotechnol.*, **2001**, 19, 365.

Elghanian R., Storhoff J.J., Mucic R.C., Letsinger R.L., and Mirkin C.A., *Science*, **1997**, 277, 1078.

Gardner K.H. and Theis T.L., *J. Colloid Interface Sci.*, **1996**, 180, 162-173.

Geoghegan W.D. and Ackerman G.A., *J. Histochem. Cytochem.*, **1977**, 25 (11), 1187.

Langevin P., *C. R. Acad. Sci. Paris*, **1908**, 146, 530.

Lin L., Zhao H.Q., Li J.R., Tang J.A., Duan M.X., and Jiang L., *Biochem. Biophys. Res. Commun.*, **2000**, 274, 817.

Lin B., Sureshkumar R., and Kardos J.L., *Ind. Eng. Chem. Res.*, **2002**, 41, 1189.

Lyon L.A., Musick M.D., and Natan M.J., *Anal. Chem.*, **1998**, 70 (24), 5177.

Morris R.E. and Saenlinger C.B., *J. Histochem. Cytochem.*, **1984**, 32, 124.

Mucic R.C., Storhoff J.J., Mirkin C.A., and Letsinger R.L., *J. Am. Chem. Soc.*, **1998**, 120 (48), 12674.

O'Daly J.P., Henkens R.W., Zhan J., and Zhang H., *U.S. Patent 5,391,272*, **1995**.

Park S.J., Taton T.A., and Mirkin C.A., *Science*, **2002**, 295, 1503.

Patolsky F., Ranjit K.T., Lichtenstein A., and Willner I., *Chem. Commun.*, **2000**, (12), 1025.

Powell R.D., Halsey C.M.R., Spector D.L., Kaurin S.L., McCann J., and Hainfield J.F., *J. Histochem. Cytochem.*, **1997**, 45 (7), 947.

Seelenbinder J.A., Brown C.W., Pivarnik P., and Rand A.G., *Anal. Chem.*, **1999**, 71 (10), 1963.

Slot J.W. and Geuze H.J., *European J. Cell Biol.*, **1985**, 38, 87.

Storhoff J.J., Elghanian R., Mucic R.C., Mirkin C.A., and Letsinger R.L., *J. Am. Chem. Soc.*, **1998**, 120 (9), 1959.

Verwey E.J.W. and Overbeek J.T.G., *Theory of the stability of lyophobic colloids*, ed. Elsevier, New York, USA, **1948**.

Weisbecker C.S., Merritt M.V., and Whitesides G.M., *Langmuir*, **1996**, 12 (16), 3763.

Zhao H.Q., Lin L., Li J.R., Tang J.A., Duan M.X., and Jiang L., *J. Nanoparticle Res.*, **2001**, 3, 321.

Abbreviations

antidig: antidigoxigenin

BSA: bovine serum albumin

CCD: charge-coupled device

dig: digoxigenin

DLVO: Derjaguin - Landau - Verwey - Overbeek

DNA: deoxyribonucleic acid

EDC: 1-ethyl-3-(3-dimethylaminopropyl)carbodiimide hydrochloride

EDTA: ethylenediaminetetraacetic acid

ELONA: enzyme-linked oligonucleotide assay

FITC: fluorescein-isothiocyanate

FRET: fluorescence resonance energy transfer

HRP: horseradish peroxidase

ME: mercaptoethanol

PEG: polyethylene glycol

PEI: polyethylene imine

pI: isoelectric point

SAM: self-assembled monolayer

SN: supernatant

SSC: saline-sodium citrate

TMB: 3,3',5,5'-tetramethyl-benzidine

tris-HCl: tris[hydroxymethyl]aminomethane hydrochloride